

Diradicals

Reaction of Paramagnetic Synthron, Lithiated 4,4,5,5-Tetramethyl-4,5-dihydro-1H-imidazol-1-oxyl 3-oxide, with Cyclic Aldonitrones of the Imidazole Series

Svyatoslav E. Tolstikov,^[a] Evgeny V. Tretyakov,^{*,[b, c]} Dmitry E. Gorbunov,^[c, d] Irina F. Zhurko,^[b, c] Matvey V. Fedin,^[a, c] Galina V. Romanenko,^[a] Artem S. Bogomyakov,^[a] Nina P. Gritsan,^[c, d] and Dmitry G. Mazhukin^{*,[b, c]}

Abstract: It was shown that dipole-stabilized paramagnetic carbanion lithiated 4,4,5,5-tetramethyl-4,5-dihydro-1H-imidazol-1-oxyl 3-oxide can be attached in a nucleophilic manner to either isolated or conjugated aldonitrones of the 2,5-dihydroimidazole 3-oxide and 2H-imidazole 1-oxide series to afford adducts the subsequent oxidation of which leads to polyfunctional mono- and diradicals. According to XRD, at least two polymorphic modifications can be formed during crystallization of the resulting paramagnetic compounds, and for each of them, geometric parameters of the mole-

cules are similar. An EPR spectrum of the diradical in frozen toluene has a complicated lineshape, which can be fairly well reproduced by using X-ray diffraction structural analysis and the following set of parameters: $D = 14.9$ mT, $E = 1.7$ mT; tensor $a(^{14}\text{N}) = [0.260 \ 0.260 \ 1.625]$ mT, two equivalent tensors for the nitronyl nitroxide moiety $a(^{14}\text{N}) = [0.198 \ 0.198 \ 0.700]$ mT, and $g \approx 2.007$. According to our DFT and ab initio calculations, the intramolecular exchange in the diradical is very weak and most likely ferromagnetic.

Introduction

Methods of site-selective nucleophilic functionalization of $\text{C}(\text{sp}^2)\text{--H}$ bonds have become an effective and universal tool in synthetic organic chemistry. The use of such an approach has allowed researchers to increase the atomic efficiency of reactions, reduce the number of steps, and avoid the introduction of various auxiliary groups or the utilization of supplementary reagents and catalysts.^[1,2] A good example of this type of transformation is the synthesis of functionally substituted nitronyl (NN) and iminonitroxyl (IN) radicals by interaction of the lithium derivative of 4,4,5,5-tetramethyl-4,5-dihydro-1H-imida-

zol-1-oxyl 3-oxide^[3-5] (**1**; see Scheme 1) with activated heteroarenes and cyclic six-membered dinitrones. Aside from the convenience of the direct introduction of a stable radical group into an unsaturated system, many of the synthesized paramagnetic compounds are unique and cannot be obtained by any other known methods.^[6,7] The present work continues this research and is focused on analysis of the products isolated from the reactions of radical **1** with cyclic aldonitrones of the imidazole series that contain either a conjugated or isolated nitrone group, compounds **2** and **4**,^[8] respectively. The latter, which also contains a nitroxyl group, is notable because when it is in a reaction both its electrophilic and nucleophilic components contain paramagnetic groups; this situation has not been described previously in the literature. The only close analogy of such a process may be the formation of a vicinal diradical by the reaction of two equivalents of compound **1** with quinoxaline 1,4-dioxide.^[4] Another interesting characteristic of aldonitrones **2** and **4** is their "dual" nature (Umpolung character), which means that in the presence of strong bases, they can generate dipole-stabilized organolithium intermediates^[9,10] that are capable of reacting further with either the excess of the un-ionized substrate (to form dimeric structures)^[11] or an extraneous electrophilic reagent that was added to the reaction.^[10] These circumstances make the reaction of lithium derivative **1** with aldonitrones of the imidazole series a rather serious challenge for a researcher.

[a] Dr. S. E. Tolstikov, Prof. M. V. Fedin, Prof. G. V. Romanenko, Dr. A. S. Bogomyakov
International Tomography Center, 3a Institutskaya Str.,
Novosibirsk 630090 (Russia)

[b] Prof. E. V. Tretyakov, I. F. Zhurko, Dr. D. G. Mazhukin
N. N. Vorozhtsov Institute of Organic Chemistry
9 Ac. Lavrentiev Avenue, Novosibirsk 630090 (Russia)
E-mail: tev@tomo.nsc.ru
dimok@nioch.nsc.ru

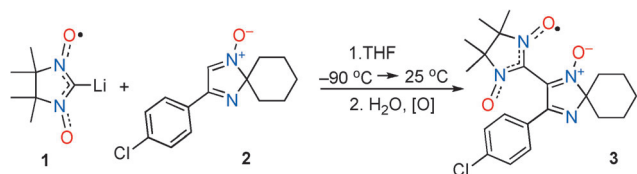
[c] Prof. E. V. Tretyakov, D. E. Gorbunov, I. F. Zhurko, Prof. M. V. Fedin, Prof. N. P. Gritsan, Dr. D. G. Mazhukin
Novosibirsk State University, 2 Pirogova Str.,
Novosibirsk 630090 (Russia)

[d] D. E. Gorbunov, Prof. N. P. Gritsan
V. V. Voevodsky Institute of Chemical Kinetics and Combustion
3 Institutskaya Str., Novosibirsk 630090 (Russia)

Supporting information for this article can be found under
<http://dx.doi.org/10.1002/chem.201602049>.

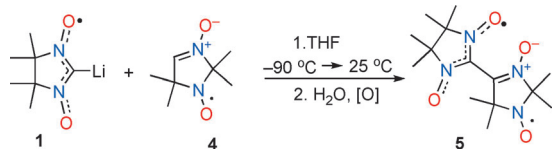
Results and Discussion

Our experiments revealed that interaction of lithium derivative **1** with aldonitrone **2** leads to the formation of a mixture of diverse products, from which target product **3** could be isolated in approximately 10% yield (Scheme 1). The oxidation of the intermediate dihydro adduct, which appears during the transformation of compound **2** into **3**, could be performed by nitroxyl radicals that were present in the reaction mixture. Indirect evidence for this was the presence (according to the chromatography–mass spectrometry) of compounds with molecular masses that corresponded to the products of deoxygenation of compounds **1** and **3**, which includes the identified 4,4,5,5-tetramethylimidazolidine, in the reaction mixture.



Scheme 1. Synthesis of nitronyl nitroxide **3**.

The reaction between compounds **1** and **4** (Scheme 2) proceeded similarly, in terms of formation of a multitude of deoxygenated products, and as a result, isolation of the desired diradical **5** was achieved in only a low yield ($\approx 10\%$). Therefore, we attempted to increase the yield of product **5** in the following ways: 1) use of an excess of substrate **1**, 2) addition of ancillary oxidants (chloranil, MnO_2) to the reaction mixture, or 3) changing the order of the reagent's addition; unfortunately, none of these approaches were successful.



Scheme 2. Synthesis of diradical **5**.

The structures of the resulting paramagnetic compounds **3** and **5** were studied by X-ray diffraction (XRD) and spectroscopic methods. We found that nitroxide **3** crystallizes in at least two polymorphic modifications: rhombic (**3a**) and triclinic (**3b**), with one and two (**3b-1** and **3b-2**) crystallographically independent molecules, respectively (Figures 1 and 2). The lengths of C–C and C–N bonds in both molecules are almost identical, whereas the lengths of N–O bonds are in the range 1.258(2)–1.277(3) Å. All molecules differ by the angle between the planes of the nitronyl nitroxide moiety and the 2*H*-imidazole cycle, which are 61.7, 49.5, and 29.5° for molecules **3a**, **b-1**, and **b-2**, respectively.

The magnitudes of the angles between the planes of the 2*H*-imidazole cycle and the benzene ring also differ substantially (Table 1). The shortest intermolecular $\text{O}_{\text{NN}^{\cdot-}}\text{O}_{\text{NN}}$ distance in

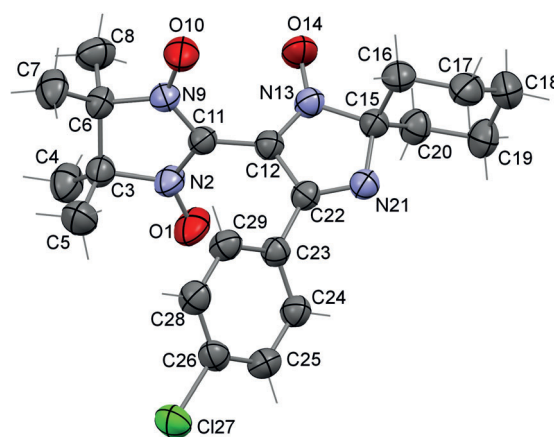


Figure 1. Structure of molecule **3** (rhombic modification).

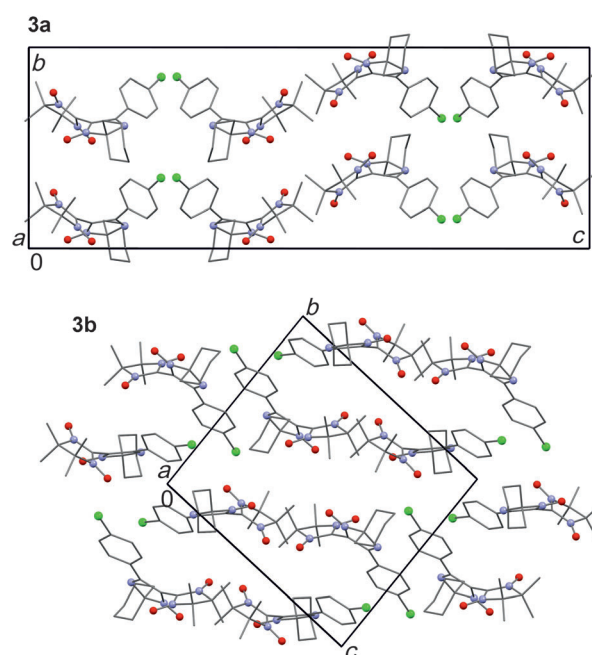


Figure 2. Packing of molecules in modifications **3a** and **b**.

compound **3a** is 4.268(3) Å, whereas in **3b**, this distance exceeds 4.6 Å. Analysis of the magnetic properties of the polymorphs **3a** and **3b** revealed that the μ_{eff} value at 300 K equaled 1.75 μ_{B} and did not change with a decrease in temperature down to 2 K. This behavior of the $\mu_{\text{eff}}(T)$ dependences indicates the absence of any meaningful exchange interactions between unpaired electrons; this notion is consistent with fairly long distances between the paramagnetic centers of radical **3** in the solid state and agrees satisfactorily with results of DFT calculations for **3a** ($J = -2.4$ K).

Diradical **5** was also isolated in two polymorphs: triclinic (**5a**) and monoclinic (**5b**), with one and two (**5b-1** and **5b-2**) crystallographically independent molecules, respectively. Bond lengths and interplane angles in various modifications of the compound do not differ significantly. Figures 3 and 4 show the structure of the triclinic modification of the diradical and the

Parameter	3 a	3 b-1	3 b-2
Bond	d [Å]	d [Å]	d [Å]
O(1)–N(2)	1.277(3)	1.258(2)	1.268(3)
N(9)–O(10)	1.271(3)	1.272(3)	1.272(3)
N(13)–O(14)	1.261(2)	1.258(2)	1.266(2)
O(10)···O(14) intramolecular	3.292(3)	2.874(2)	3.041(2)
O···O intermolecular	4.268(3)	> 4.6	
Angle	ω [°]	ω [°]	ω [°]
\angle {N(2)C(11)N(9)}–{N(13)C(12)C(22)}	61.7	49.5	29.5
\angle {Ar}–{C(12)C(22)N(21)}	50.3	40.6	11.1

packing arrangements of the molecules in crystals of polymorphs **5 a** and **5 b**. By means of the shortest alternating distances between O atoms of neighboring molecules ($O\cdots O = 3.878(4)$, $3.892(4)$ Å) in the structure of **5 a**, it was possible to identify chains that extend longitudinally [100], whereas in structure **5 b**, one could only distinguish the pairs of molecules with noticeably greater $O\cdots O$ distances ($4.054(4)$ and $4.454(4)$ Å) (Table 2).

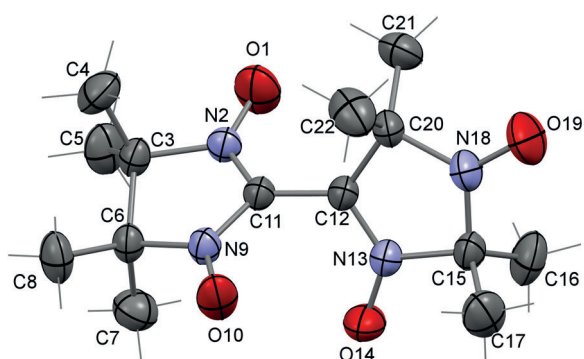


Figure 3. Structure of the diradical **5** (triclinic polymorph **5 a**).

At room temperature, the solution-state EPR spectrum of nitronyl nitroxide radical **3** in toluene was simulated by using two equivalent nitrogen HFI constants $a(^{14}\text{N}) = 0.72$ mT (Figure 5a). For the optimized geometry of radical **3**, calculations predicted similar HFI constants for both nitrogen atoms of the nitronyl nitroxide unit ($a_{\text{calcd}}(^{14}\text{N}) = 0.50$ and 0.48 mT). The lineshape had comparable contributions from Lorentzian ($\Gamma_{\text{pp}} = 0.3$ mT) and Gaussian ($\Gamma_{\text{pp}} = 0.2$ mT) broadening, and further dilution did not allow us to resolve other HFI constants, for example $a_{\text{calcd}}(^{14}\text{N}) = -0.11$ mT (nitron fragment). Thus, it is reasonable to assume that this and other smaller HFIs contribute to the inhomogeneous broadening of the spectrum.

In the case of diradical **5**, the room-temperature EPR spectrum in toluene solution was poorly resolved (Figure 5b). The diradical is quite rigid, therefore the rotation of its monoradical moieties is low, even in solution, to produce the isotropic spectra with well-resolved EPR lines. At the same time, dipolar coupling might not be fully averaged by a rotation of the whole diradical, and its residual presence should lead to line broaden-

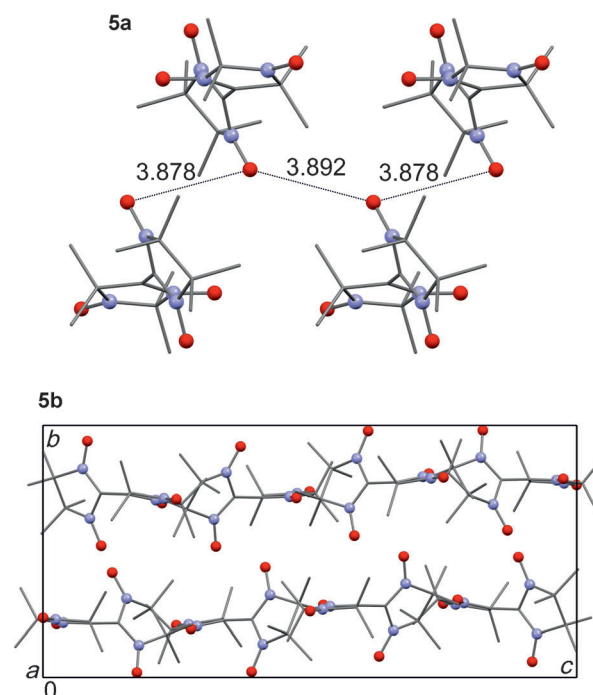


Figure 4. Packing of molecules in modifications **5 a** and **b**.

Parameter	5 a	5 b-1	5 b-2
Bond	d [Å]	d [Å]	d [Å]
O(1)–N(2)	1.270(2)	1.271(3)	1.247(3)
N(9)–O(10)	1.271(2)	1.274(3)	1.268(3)
N(13)–O(14)	1.270(2)	1.270(3)	1.264(3)
N(18)–O(19)	1.271(2)	1.274(3)	1.262(3)
O(10)···O(14) intramolecular	3.066(3)	3.192(3)	3.241(4)
O···O intermolecular	3.878(4), 3.892(4)	4.054(4), 4.454(4)	
Angle	ω [°]	ω [°]	ω [°]
\angle {N(2)C(11)N(9)}–{N(13)C(12)C(20)}	61.0	67.4	68.3

ing, as is observed experimentally (Figure 5b). The line broadening was fully avoided by dilution, but the spectral resolution was still insufficient for obtaining quantitative information.

The EPR spectrum of the diradical **5** in frozen toluene (at 80 K) is better resolved and has a complicated lineshape determined by the zero-field splitting (ZFS) and three ^{14}N HFIs (Figure 6). Simulation of such a system with generally rhombic ZFS (D -tensor) and anisotropic HFIs (A -tensors) that are tilted with respect to each other is rather difficult; even so, we achieved reasonably good agreement with the experimental data, as shown in Figure 6. We used the XRD structure to choose relative directions of D - and A -tensors. For simplicity's sake, we assumed that the D -tensor has a purely dipolar origin, and therefore, it is orientated along the approximate direction between the two radical centers (centers of electron density distributions). ^{14}N HFI tensors were assumed to be orientated as usual for the corresponding types of radicals (the x -axis is

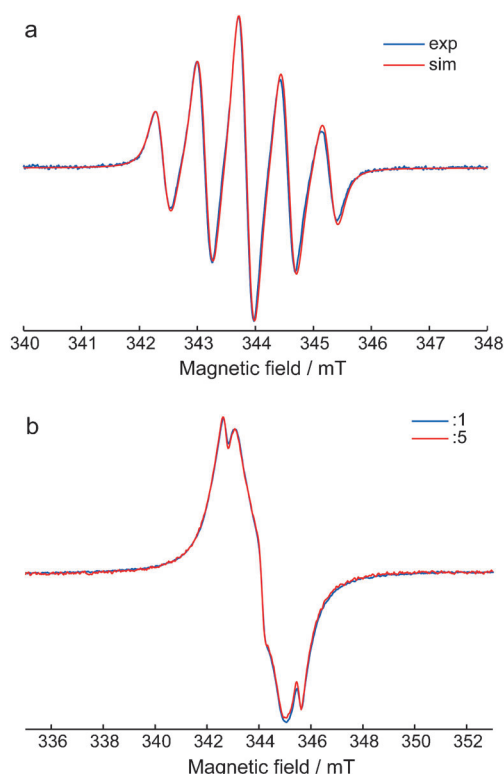


Figure 5. a) Room-temperature X-band EPR spectrum of nitronyl nitroxide **3** in toluene ($\nu_{mw} \approx 9.659$ GHz), and the simulation obtained by using two equivalent isotropic HFI constants $a(^{14}\text{N}) = 0.72$ mT. b) Room-temperature X-band EPR spectra of diradical **5** in toluene ($\nu_{mw} \approx 9.658$ GHz) for two concentrations of diradical that differ by a factor of 5 ν/ν (indicated as “1” and “5”).

along the N–O[•] bond, and the z-axis is perpendicular to the plane of the CN–O[•] fragment). The following set of parameters was used for the simulation that is shown in Figure 6: ZFS parameters $D = 14.9$ mT and $E = 1.7$ mT, HFI tensor for the “isolated” nitroxide group $a(^{14}\text{N}) = [0.260 \ 0.260 \ 1.625]$ mT, two equivalent tensors for the nitronyl nitroxide moiety $a(^{14}\text{N}) = [0.198 \ 0.198 \ 0.700]$ mT, and $g \approx 2.007$.

The ZFS parameters that were used for the simulation were in good agreement with those calculated at the DFT level for the optimized geometry of diradical **5**: $D = -16.2$ mT and $E = -1.5$ mT (see the Supporting Information, Table S1). The calculated ^{14}N HFI values were roughly two times larger than those obtained from the simulations of EPR data: $a_{\text{calcd}}(^{14}\text{N}) = [-0.55 \ -0.52 \ 2.23]$ mT for the “isolated” nitroxide group, and two similar tensors, $a_{\text{calcd}}(^{14}\text{N}) = [-0.31 \ -0.29 \ 1.29]$ and $[-0.33 \ -0.30 \ 1.34]$ mT, for the nitronyl nitroxide moiety (see the Supporting Information, Table S2). The observation of HFI constants in the diradicals that were two times smaller than the corresponding monoradical fragments is characteristic for the systems with strong intramolecular spin–spin interaction $|J| \gg a(^{14}\text{N})$. Note that it is impossible to determine the signs of the A and b-tensor components from X-band EPR data.

Examination of magnetic characteristics of structure **5a** revealed that, at 300 K, the μ_{eff} value was $2.41 \mu_{\text{B}}$ (Figure 7), which is in good agreement with the theoretical value ($2.45 \mu_{\text{B}}$) for two non-interacting paramagnetic centers with spins

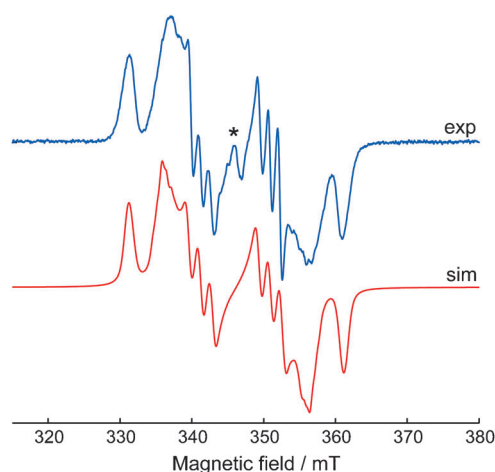


Figure 6. X-band EPR spectra of nitronyl nitroxide **5** in toluene ($\nu_{mw} \approx 9.697$ GHz) at 80 K, and the simulation obtained by using the parameters described in the text. The asterisk marks a small admixture of the monoradical at the center of the spectrum.

$S = 1/2$ at the g-factor of 2. If the temperature was lowered to 100 K, μ_{eff} hardly changed, but it decreases to $1.77 \mu_{\text{B}}$ at 2 K, which corresponds to the disappearance of half of the spins in the system. To elucidate these phenomena at the molecular level and to conduct a correct simulation of the magnetic properties of compound **5**, the intra- and intermolecular exchange interactions were calculated for the XRD structures.

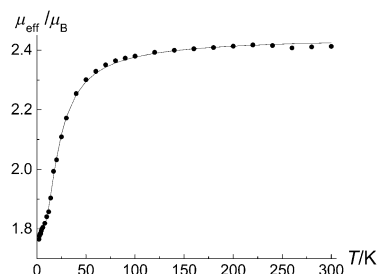


Figure 7. Experimental (●) and theoretical (solid line) $\mu_{\text{eff}}(T)$ dependences for compound **5a**.

The DFT calculations predicted that in diradicals **5a**, **5b-1**, and **5b-2**, the intramolecular exchange interactions are weak and ferromagnetic in nature and are characterized by $J = 5.0$, 5.0 , and 5.1 K, respectively. Diradical **5** can be classified as a disjoint-type diradical because the SOMO orbitals are confined in different regions of space. Previously, we demonstrated that, for similar diradicals, DFT calculations overestimate the ferromagnetic contribution to exchange interactions;^[12] therefore, we also performed the CASSCF(10,8) and NEVPT2(10,8) calculations, which predicted the values of $J = 0.0$ and $+2.1$ K, respectively, for diradical **5a** (see the Supporting Information, active space is presented in Figure S1). Thus, diradicals **5a** and **5b** are characterized by extremely weak and most likely ferromagnetic exchange interactions. Obviously, the decrease of μ_{eff}

below 100 K is caused by strong antiferromagnetic intermolecular exchange interactions.

The XRD analysis of diradical **5a** was suggestive of some intermolecular spin pairing because of the short intermolecular distances between the O atoms of the nitronyl nitroxides. To estimate parameters of the intermolecular exchange interactions, we performed calculations for neighboring diradicals by taking into account only one radical fragment from each molecule. Such estimations are correct for disjoint-type diradicals (see the Supporting Information, Figure S2).^[12] For diradical **5a**, the magnetic interactions that arise from the shortest $O_{NN^{\bullet}}\cdots O_{NN}$ intermolecular contacts (3.783 Å) were predicted to be strongly antiferromagnetic ($J_{\text{calcd}}/k_B = -16.6$ K). Another short $O_{NN^{\bullet}}\cdots O_{NN}$ intermolecular contact (3.892 Å) yielded much weaker exchange interactions ($J_{\text{calcd}}/k_B = -2.9$ K). All other intermolecular interactions were estimated to be negligible ($|J_{\text{calcd}}|/k_B < 0.1$ K). Taking into account only one type of exchange interaction, namely the strongest interaction of radical fragments with the shortest contact ($R_{O\cdots O} = 3.783$ Å), the temperature dependence of the effective magnetic moments was approximated by using the Bleaney–Bowers equation^[13] for exchange-coupled moieties and the Curie–Weiss law for non-interaction ones (Figure 7). The best agreement with the experimental data was achieved at the values of J/k_B , g -factor, and monomer admixture p , which were equal to -23 K, 2.06, and 0.02, respectively. The former J/k_B value (-23 K) coincided well with the calculations, $J_{\text{calcd}}/k_B = -16.6$ K, which supports the proposed simplified model.

As aforementioned, the noticeably longer $O\cdots O$ distances were identified for diradical **5b**. In accordance with this observation, calculations for diradical **5b** predict only weak and mainly antiferromagnetic interactions, $|J_{\text{calcd}}|/k_B \leq 1.2$ K.

Conclusions

Our results show that paramagnetic lithium derivative **1** reacts with cyclic five-membered nitrones, including those containing a nitroxide group, and this reaction leads to new polyfunctional nitroxides. The compact diradical **5**, which in contrast to previously obtained isomeric bis-nitronyl nitroxide **6**,^[14] contains nitroxide groups of different types, is kinetically stable and has a T-shape topology. To the best of our knowledge, there is only one example of the synthesis of stable nitroxyl diradical **7** that possesses a similar topology; this diradical contains 2-imidazoline and 3-pyrroline moieties (Figure 8). The compound was obtained by the condensation of 2,3-bis(hydroxyamino)-2,3-dimethylbutane sulfate with the 3-formyl derivative of 2,5-dihydropyrrole followed by the sequential, selective oxidation of N–OH and NH groups.^[15] Structural characteristics of hetero diradical **7** are similar to those of diradical **5**, except for the difference in the torsion angle between the heterocycles ($\approx 18.2^\circ$ versus $\approx 65^\circ$), which can be explained by the effect of dipole–dipole repulsion of the two electron acceptor moieties N^+-O^- . This difference appeared to be crucial for the value of exchange interaction between unpaired electrons. According to the quantum chemical calculations at the NEVPT2/SVP level (see the Supporting Information, Table S3),

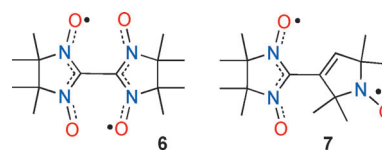


Figure 8. Previously reported diradicals **6** and **7**.

the diradical **7** has the triplet ground state with a noticeable $J = 10.9$ K (see the Supporting Information, Figure S3). The intermolecular exchange interactions in the crystal of diradical **7** were also predicted to be perceptible and antiferromagnetic (see the Supporting Information, Figure S4).

The intramolecular exchange in diradical **5** is very weak and most likely ferromagnetic; the diradical **7** is definitely characterized by substantial ferromagnetic exchange interaction. Both diradicals contain a new type of ferromagnetically coupled unit, which can be used for the construction of stable molecules with the high-spin ground state. Apart from this, both diradicals and their derivatives are of great importance as building blocks in the molecular design of heterospin, magnetically active systems and for the creation of magnetically active electrochemical labels.

Experimental Section

General procedures

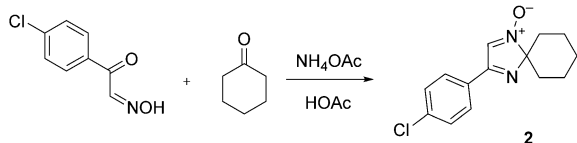
4,4,5,5-Tetramethyl-4,5-dihydro-1H-imidazol-1-oxyl 3-oxide was synthesized in accordance with a literature procedure.^[6] Aldonitrone **4** was obtained in two steps from 2-hydroxyamino-2-methylpropanal oxime^[16] in accordance with a previously described method^[17] with a minor modification, which enabled an increase in the yield of intermediate 1-hydroxy-3-imidazoline **8** (see below). THF was distilled from sodium benzophenone ketyl in a recycling still. Other reagents and solvents from commercial sources were of the highest purity available and used as received. Reactions were monitored by thin-layer chromatography (TLC) on a precoated plate of silica gel (Silica gel 60 F₂₅₄, Merck). Column chromatography was performed on silica gel 60 (220–240 mesh).

NMR spectra were recorded on an Avance-400 (400.13 MHz for ^1H and 100.62 MHz for ^{13}C) spectrometer; deuteriochloroform (CDCl_3) was used as solvent, with residual CHCl_3 ($\delta_{\text{H}} = 7.26$ ppm) or CDCl_3 ($\delta_{\text{C}} = 77.0$ ppm) serving as internal standards. The FT-IR spectra were recorded on a Vector-22 instrument for samples pelleted with KBr (0.25%). The UV/Vis absorption spectra were taken on a spectrophotometer Hewlett Packard 4853. Elemental analysis was carried out in a Carlo Erba automatic C, H, N-analyzer model 1106. For EPR investigation, the compounds were dissolved in toluene, placed in the quartz tubes, and studied by using a Bruker Elexsys E580 spectrometer in CW mode at X-band (9 GHz), either at 300 or 80 K. Simulations of EPR data were done by using EasySpin.^[18] The magnetic susceptibility of the polycrystalline samples was measured with a Quantum Design MPMSXL SQUID magnetometer in the temperature range 2–300 K with the magnetic field of up to 5 kOe. None of the samples showed any field dependence of molar magnetization at low temperatures. Diamagnetic corrections were made by using the Pascal constants. The effective magnetic moment was calculated as $\mu_{\text{eff}}(T) = [(3k/N_A\mu_B^2)\chi T]^{1/2} \approx (8\chi T)^{1/2}$.

Organic syntheses

3-(4-Chlorophenyl)-1,4-diaza-spiro[4.5]deca-1,3-diene 1-oxide **2**

(**2**): Compound **2** was prepared by the condensation of 2-(4-chlorophenyl)-2-oxoacetaldehyde oxime with cyclohexanone and ammonium acetate in accordance with a published procedure^[19] (Scheme 3).



Scheme 3. Condensation of 2-(4-chlorophenyl)-2-oxoacetaldehyde oxime with cyclohexanone.

A mixture of 2-(4-chlorophenyl)-2-oxoacetaldehyde oxime (1.83 g, 10 mmol), cyclohexanone (7.8 mL, 75 mmol), ammonium acetate (4.6 g, 60 mmol), and acetic acid (5 mL) was stirred at 20 °C for 14 h. The mixture was diluted with water (50 mL), extracted with chloroform, and washed with 2 M aqueous NaOH. The organic phase was dried with MgSO₄, isolated by filtration, and concentrated under vacuum. The residue was triturated with diethyl ether, and after filtration and recrystallization (ethyl acetate/hexane, 1:1), the product **2** (1.23 g, 47%) was isolated as a colorless solid. m.p. 140–142 °C; ¹H NMR (400 MHz, CDCl₃): δ = 1.40 (m, 3 H, (CH₂)₅), 1.85 (m, 5 H, (CH₂)₅), 2.07 (m, 2 H, (CH₂)₅), 7.41, 7.79 (d, AA'BB', *J* = 8.5 Hz; both 2 H, Ar), 7.67 ppm (s, 1 H, H–C₂); ¹³C NMR (100 MHz; CDCl₃): δ = 23.2, 23.1, 34.9 ((CH₂)₅), 104.7 (C₅), 124.8 (C₂), 128.3 (*ortho*-C, Ar), 129.0 (*meta*-C, Ar), 129.9 (*ipso*-C, Ar), 137.5 (C–Cl), 163.4 ppm (C₃); IR (KBr): $\tilde{\nu}$ = 3067, 2935, 2859, 1602, 1587, 1558, 1508, 1486, 1448, 1417, 1378, 1297, 1260, 1232, 1167, 1089, 1066, 1015, 984, 949, 912, 871, 853, 831 cm⁻¹; UV/Vis (EtOH): λ_{max} (log ε) = 243 (4.19), 278 nm (4.19); elemental analysis calcd (%) for C₁₄H₁₅ClN₂O (262.74): C 64.0, H 5.8, Cl 13.5, N 10.7; found: C 63.9, H 5.6, Cl 13.5, N 10.8.

2-(3-(4-Chlorophenyl)-1-oxido-1,4-diazaspiro[4.5]deca-1,3-dien-2-yl)-4,4,5,5-tetramethyl-4,5-dihydro-1H-imidazol-1-oxyl 3-oxide **3**

(**3**): A 1.0 M solution of LiN(SiMe₃)₂ in THF (1.1 mL, 1.1 mmol) was added to an actively stirring solution of 4,4,5,5-tetramethyl-4,5-dihydro-1H-imidazol-1-oxyl 3-oxide (157 mg, 1.0 mmol) in anhydrous THF (30 mL) at –90 °C under an argon atmosphere, and the stirring was continued for 30 min. A solution of nitron **2** (223 mg, 1.0 mmol) in THF (10 mL) at –90 °C was added dropwise, and the mixture was allowed to warm gradually to room temperature in a bath. The reaction mixture was poured into a Petri dish and left in the open air until complete evaporation of the solvent. The residue was subjected to column chromatography on SiO₂ (EtOAc). The fraction that contained the target product was concentrated under vacuum, and the residue was recrystallized (Et₂O/*n*-heptane) to yield the product **3** (38 mg, 9%) as needle-like dark green crystals. *R*_f = 0.67 (EtOAc); m.p. 177.5–177.6 °C; IR (KBr): $\tilde{\nu}$ = 3043, 3001, 2989, 2949, 2943, 2858, 1605, 1585, 1564, 1508, 1483, 1448, 1423, 1373, 1336, 1292, 1269, 1219, 1176, 1163, 1136, 1086, 1066, 1011, 1001, 958, 906, 841, 746, 737, 685, 615, 540, 490, 465 cm⁻¹; UV/Vis (CHCl₃): λ_{max} (log ε) = 263 (4.26), 327 (4.11), 409 sh. (3.27), 567 nm (2.48); elemental analysis calcd (%) for C₂₁H₂₆ClN₄O₃ (417.91): C 60.4, H 6.3, N 13.4; found: C 60.3, H 6.1, N 13.5.

1-Hydroxy-2,2,5,5-tetramethyl-2,5-dihydro-1H-imidazole 3-oxide **8**: Finely powdered 2-hydroxyamino-2-methylpropanal oxime (4.720 g, 40 mmol) was mixed with freshly distilled 2,2-diethoxy-

propane (8.450 g, 64 mmol) in a round-bottomed flask, and glacial AcOH (2.280 mL, 40 mmol) was added dropwise to the stirring mixture until a thick slurry had formed. The flask was equipped with the Dean–Stark trap, immersed into a preheated oil bath (125 °C), and stirred until complete dissolution of the precipitate (≈ 1 min). The mixture was heated at reflux for 25 min, over which time the oil bath temperature was constantly decreased from 120 to 112 °C; the reaction mixture was eventually cooled in an ice bath to induce abundant precipitation of the product. The suspension was diluted with dry diethyl ether (7 mL) and kept in a freezer (–18 °C) for 12 h. The precipitate was isolated by filtration and washed twice with cool diethyl ether to obtain 1-hydroxy-3-imidazoline 3-oxide **7** (3.289 g, 52%) as colorless crystals. m.p. 172–174 °C (lit. m.p. 172–174 °C^[17]).

2,2,5,5-Tetramethyl-2,5-dihydro-1H-imidazol-1-oxyl 3-oxide **4**: Compound **4** was prepared by oxidation of compound **8** with MnO₂ in chloroform.^[17]

2',2',4,4,5,5,5',5'-Octamethyl-2',4,5,5'-tetrahydro-1H,1'H-2,4'-biimidazol-1,1'-bioxyl 3,3'-dioxide **5**: A 1.0 M solution of LiN(SiMe₃)₂ in THF (2.8 mL, 2.8 mmol) was added to an actively stirring solution of 4,4,5,5-tetramethyl-4,5-dihydro-1H-imidazol-1-oxyl 3-oxide (400 mg, 2.54 mmol) in anhydrous THF (30 mL) at –90 °C under an argon atmosphere, and the stirring was continued for 30 min. The resulting solution was added dropwise to a solution of compound **4** (400 mg, 2.54 mmol) in THF (20 mL) at –90 °C, and the mixture was left in a bath to warm gradually to room temperature. The reaction mixture was poured into a Petri dish and left in the open air until complete evaporation of the solvent. The residue was subjected to column chromatography on SiO₂ (EtOAc). The fraction that contained the target product was concentrated, and the residue was recrystallized (CH₂Cl₂/*n*-heptane) to yield the product **5** (62 mg, 8%) as dark green crystals; *R*_f = 0.63 (EtOAc); m.p. 137.1–137.7 °C; IR (KBr): $\tilde{\nu}$ = 3433, 2990, 2932, 1558, 1520, 1458, 1437, 1423, 1377, 1367, 1354, 1308, 1281, 1254, 1219, 1196, 1169, 1140, 1094, 870, 853, 690, 598, 581, 555, 538, 465, 417 cm⁻¹; UV/Vis (MeOH): λ_{max} (log ε) = 220 (3.82), 277 (3.90), 361 sh. (3.64), 375 nm (3.70); elemental analysis calcd (%) for C₁₄H₂₄N₄O₄ (312.37): C 53.8, H 7.7, N 17.9; found: C 53.8, H 7.5, N 17.8.

X-ray crystallography

Perfect crystals of nitroxides **3** and **5** were grown from a mixture of CH₂Cl₂ with *n*-heptane. The diffraction reflections from the stand-alone crystals were registered on a SMART APEX II CCD (Bruker AXS) diffractometer (Mo_{Kα}, λ = 0.71073 Å) and APEX DUO (Cu_{Kα}, λ = 1.54178 Å). An absorption correction was included in the Bruker SADABS software (version 2.10). The structures were solved by direct methods and refined by full-matrix least-squares analysis in an anisotropic approximation for all nonhydrogen atoms. The positions of H atoms were calculated geometrically and refined isotropically in a rigid group approximation. All calculations on structure solution and refinement were performed in the Bruker Shelxtl software, version 6.14. Crystal data and selected bond lengths and angles are listed in Tables 1 and 2.

CCDC 1468149 (**3a**), 1468150 (**3b**), 1468151 (**5a**), and 1468152 (**5b**) contain the supplementary crystallographic data for this paper. These data are provided free of charge by The Cambridge Crystallographic Data Centre.

Compound 3a: C₂₁H₂₆ClN₄O₃; *FW* = 417.91, *T* = 296 K, orthorhombic, *Pbca*, *a* = 10.3881(15), *b* = 12.0820(16), *c* = 33.683(4) Å, *V* = 4227.5(9) Å³, *Z* = 8, *D*_{calcd} = 1.313 g cm⁻³, μ(Cu Kα) = 1.845 mm⁻¹, a total of 25 445 (θ_{max} = 67.565°), 3766 unique (*R*_{int} = 0.0574), 2768 (*I* > 2σ), 263 parameters. Goof = 1.025, *R*₁ = 0.0486, *wR*₂ = 0.1282

($I > 2\sigma$), $R1 = 0.0695$, $wR2 = 0.1439$ (all data), $\max m^{-1}$ diff. peak $0.255/-0.195 \text{ e}\text{\AA}^{-3}$.

Compound 3b: $C_{21}H_{26}ClN_4O_3$: $FW = 417.91$, $T = 296 \text{ K}$, triclinic, $P\bar{1}$, $a = 11.8920(5)$, $b = 13.8752(6)$, $c = 14.4861(6) \text{ \AA}$, $\alpha = 89.275(2)$, $\beta = 78.4195(18)$, $\gamma = 67.4196(18)^\circ$, $V = 2156.61(16) \text{ \AA}^3$, $Z = 4$, $D_{\text{calcd}} = 1.287 \text{ g cm}^{-3}$, $\mu(\text{Cu K}\alpha) = 1.808 \text{ mm}^{-1}$, a total of 31043 ($\theta_{\text{max}} = 67.411^\circ$), 7544 unique ($R_{\text{int}} = 0.0409$), 7544 ($I > 2\sigma$), 534 parameters. Goof = 1.037, $R1 = 0.0472$, $wR2 = 0.1248$ ($I > 2\sigma$), $R1 = 0.0591$, $wR2 = 0.1342$ (all data), $\max m^{-1}$ diff. peak $0.554/-0.489 \text{ e}\text{\AA}^{-3}$.

Compound 5a: $C_{14}H_{24}N_4O_4$: $FW = 312.37$, $T = 296 \text{ K}$, triclinic, $P\bar{1}$, $a = 7.505(6)$, $b = 11.012(8)$, $c = 11.446(9) \text{ \AA}$, $\alpha = 97.009(9)$, $\beta = 106.909(9)$, $\gamma = 108.531(8)^\circ$, $V = 835.3(11) \text{ \AA}^3$, $Z = 2$, $D_{\text{calcd}} = 1.242 \text{ g cm}^{-3}$, $\mu(\text{Mo K}\alpha) = 0.092 \text{ mm}^{-1}$, a total of 6179 ($\theta_{\text{max}} = 28.043^\circ$), 4260 unique ($R_{\text{int}} = 0.0579$), 2191 ($I > 2\sigma$), 200 parameters. Goof = 0.862, $R1 = 0.0559$, $wR2 = 0.1336$ ($I > 2\sigma$), $R1 = 0.1014$, $wR2 = 0.1570$ (all data), $\max m^{-1}$ diff. peak $0.209/-0.259 \text{ e}\text{\AA}^{-3}$.

Compound 5b: $C_{14}H_{24}N_4O_4$: $FW = 312.37$, $T = 296 \text{ K}$, monoclinic, $P21/c$, $a = 13.7053(6)$, $b = 10.7785(5)$, $c = 22.8303(9) \text{ \AA}$, $\beta = 89.992(3)^\circ$, $V = 3372.6(3) \text{ \AA}^3$, $Z = 8$, $D_{\text{calcd}} = 1.230 \text{ g cm}^{-3}$, $\mu(\text{Mo K}\alpha) = 0.091 \text{ mm}^{-1}$, a total of 31850 ($\theta_{\text{max}} = 28.358^\circ$), 8329 unique ($R_{\text{int}} = 0.0555$), 3150 ($I > 2\sigma$), 399 parameters. Goof = 0.764, $R1 = 0.0466$, $wR2 = 0.1121$ ($I > 2\sigma$), $R1 = 0.1599$, $wR2 = 0.1432$ (all data), $\max m^{-1}$ diff. peak $0.254/-0.297 \text{ e}\text{\AA}^{-3}$.

DFT and ab initio calculations

The spin-spin part of the D tensor was only calculated by using the approach^[20] implemented in the ORCA package.^[21] The spin-restricted open-shell DFT approach with a pure BP86 functional^[22] and def2-TZVP basis set^[23] was used for calculations of the ZFS. Calculations were performed for XRD geometry of diradicals as well as for their geometries optimized at the triplet states.

The J values in the spin-Hamiltonian ($H = -2J\cdot S_1\cdot S_2$) were calculated by using both the spin-unrestricted broken-symmetry (BS) approach^[24] at the UB3LYP/def2-TZVP level of theory^[25] and multi-reference CASSCF and CASSCF/NEVPT2 procedures^[26] with def2-SVP basis set.^[27] All calculations were performed by using ORCA suit of programs.^[20]

The HFI constants and HFI tensors were calculated at the UB3LYP/def2-TZVP level by using Gaussian09 suit of programs.^[28]

Acknowledgements

The authors thank the Russian Science Foundation (project 15-13-20020), FASO Russia (project 0333-2014-0001, 0302-2015-0002) for financial support and the Multi-Access Chemical Service Center SB RAS for spectral and analytical measurements. S.T. thanks the President of the Russian Federation Council for grants (grant No. MK-6040.2016.3) for partial support of the synthetic part of this work. The computational part of this work was supported by the RFBR project 15-03-03242.

Keywords: ab initio calculations • density functional calculations • diradicals • EPR spectroscopy • X-ray diffraction

- [1] V. N. Charushin, O. N. Chupakhin, *Pure Appl. Chem.* **2004**, *76*, 1621–1631.
 [2] I. S. Kovalev, D. S. Kopchuk, G. V. Zyryanov, V. L. Rusinov, O. N. Chupakhin, V. N. Charushin, *Russ. Chem. Rev.* **2015**, *84*, 1191–1225.
 [3] R. Weiss, N. Kraut, F. Hampel, *J. Organomet. Chem.* **2001**, *617*, 473–482.

- [4] O. N. Chupakhin, I. A. Utepova, M. V. Varaksin, E. V. Tretyakov, G. V. Romanenko, D. V. Stass, V. I. Ovcharenko, *J. Org. Chem.* **2009**, *74*, 2870–2872.
 [5] E. V. Tretyakov, V. I. Ovcharenko, *Russ. Chem. Rev.* **2009**, *78*, 971–1012.
 [6] E. V. Tretyakov, I. A. Utepova, M. V. Varaksin, S. E. Tolstikov, G. V. Romanenko, A. S. Bogomyakov, D. V. Stass, V. I. Ovcharenko, O. N. Chupakhin, *ARKIVOC* **2011**, 76–98.
 [7] M. V. Varaksin, E. V. Tretyakov, I. A. Utepova, G. V. Romanenko, A. S. Bogomyakov, D. V. Stass, R. Z. Sagdeev, V. I. Ovcharenko, O. N. Chupakhin, *Russ. Chem. Bull.* **2012**, *61*, 1469–1473.
 [8] V. V. Martin, L. B. Volodarskii, M. A. Voinov, T. A. Berezina, T. F. Lelyukh, *Russ. Chem. Bull.* **1988**, *37*, 1677–1683.
 [9] M. A. Voinov, G. E. Salnikov, A. M. Genae, V. I. Mamatyuk, M. M. Shakirov, I. A. Grigor'ev, *Magn. Reson. Chem.* **2001**, *39*, 681–683.
 [10] M. A. Voinov, T. G. Shevelev, T. V. Rybalova, Y. V. Gatilov, N. V. Pervukhina, A. B. Burdukov, I. A. Grigor'ev, *Organometallics* **2007**, *26*, 1607–1615.
 [11] M. A. Voinov, I. A. Grigor'ev, L. B. Volodarsky, *Heterocycl. Commun.* **1998**, *4*, 261–270.
 [12] S. Tolstikov, E. Tretyakov, S. Fokin, E. Suturina, G. Romanenko, A. Bogomyakov, D. Stass, A. Maryasov, N. Gritsan, V. Ovcharenko, *Chem. Eur. J.* **2014**, *20*, 2793–2803.
 [13] B. Bleaney, K. D. Bowers, *Proc. R. Soc. London Ser. A* **1952**, *214*, 451–465.
 [14] D. G. B. Boockock, E. F. Ullman, *Chem. Commun.* **1969**, 1161–1162.
 [15] T. Kálai, J. Jekó, Z. Szabó, L. Párkányi, K. Hideg, *Synthesis* **1997**, 1049–1055.
 [16] L. B. Volodarsky, A. Y. Tikhonov, *Synthesis* **1986**, 704–715.
 [17] J. F. Polienko, T. Schanding, M. A. Voinov, I. A. Grigor'ev, *Synth. Commun.* **2006**, *36*, 2763–2768.
 [18] S. Stoll, A. Schweiger, *J. Magn. Reson.* **2006**, *178*, 42–55.
 [19] I. A. Kirilyuk, I. A. Grigor'ev, L. B. Volodarskii, *Bull. Acad. Sci. USSR Div. Chem. Sci.* **1991**, *40*, 1871–1879.
 [20] a) F. Neese, *J. Am. Chem. Soc.* **2006**, *128*, 10213–10222; b) D. Ganyushin, F. Neese, *J. Chem. Phys.* **2006**, *125*, 024103.
 [21] a) F. Neese, *WIREs Comput. Mol. Sci.* **2012**, *2*, 73–78; b) F. Neese, *ORCA: An Ab Initio, Density Functional and Semiempirical Program Package, Version 2.9*, Max Planck Institute for Bioinorganic Chemistry, Mülheim, Germany, **2012**.
 [22] a) A. D. Becke, *Phys. Rev. A* **1988**, *38*, 3098–3010; b) J. P. Perdew, *Phys. Rev. B* **1986**, *33*, 8822–8824.
 [23] F. Weigend, R. Ahlrichs, *Phys. Chem. Chem. Phys.* **2005**, *7*, 3297–3305.
 [24] a) L. Noodleman, *J. Chem. Phys.* **1981**, *74*, 5737–5743; b) K. Yamaguchi, Y. Takahara, T. Fueno, in *Applied Quantum Chemistry* (Eds.: V. H. Smith, H. F. Schaefer, K. Morokuma), Reidel, Dordrecht, **1986**, pp. 155–184; c) T. Soda, Y. Kitagawa, T. Onishi, Y. Takano, Y. Shigeta, H. Nagao, Y. Yoshioka, K. Yamaguchi, *Chem. Phys. Lett.* **2000**, *319*, 223–230.
 [25] a) A. D. Becke, *J. Chem. Phys.* **1993**, *98*, 5648–5652; b) C. Lee, W. Yang, R. G. Parr, *Phys. Rev. B* **1988**, *37*, 785–789.
 [26] a) C. Angeli, R. Cimiraglia, S. Evangelisti, T. Leininger, J.-P. Malrieu, *J. Chem. Phys.* **2001**, *114*, 10252–10264; b) C. Angeli, R. Cimiraglia, J.-P. Malrieu, *J. Chem. Phys.* **2002**, *117*, 9138–9153.
 [27] A. Schaefer, H. Horn, R. Ahlrichs, *J. Chem. Phys.* **1992**, *97*, 2571–2577.
 [28] Gaussian 09, Revision D.01, M. J. Frisch, G. W. Trucks, H. B. Schlegel, G. E. Scuseria, M. A. Robb, J. R. Cheeseman, G. Scalmani, V. Barone, B. Menonucci, G. A. Petersson, H. Nakatsuji, M. Caricato, X. Li, H. P. Hratchian, A. F. Izmaylov, J. Bloino, G. Zheng, J. L. Sonnenberg, M. Hada, M. Ehara, K. Toyota, R. Fukuda, J. Hasegawa, M. Ishida, T. Nakajima, Y. Honda, O. Kitao, H. Nakai, T. Vreven, J. A. Montgomery, Jr., J. E. Peralta, F. Ogliaro, M. Bearpark, J. J. Heyd, E. Brothers, K. N. Kudin, V. N. Staroverov, T. Keith, R. Kobayashi, J. Normand, K. Raghavachari, A. Rendell, J. C. Burant, S. S. Iyengar, J. Tomasi, M. Cossi, N. Rega, J. M. Millam, M. Klene, J. E. Knox, J. B. Cross, V. Bakken, C. Adamo, J. Jaramillo, R. Gomperts, R. E. Stratmann, O. Yazyev, A. J. Austin, R. Cammi, C. Pomelli, J. W. Ochterski, R. L. Martin, K. Morokuma, V. G. Zakrzewski, G. A. Voth, P. Salvador, J. J. Dannenberg, S. Dapprich, A. D. Daniels, O. Farkas, J. B. Foresman, J. V. Ortiz, J. Cioslowski, D. J. Fox, Gaussian, Inc., Wallingford CT, **2013**.


Received: May 2, 2016
 Published online on ■■■ ■■■, 0000

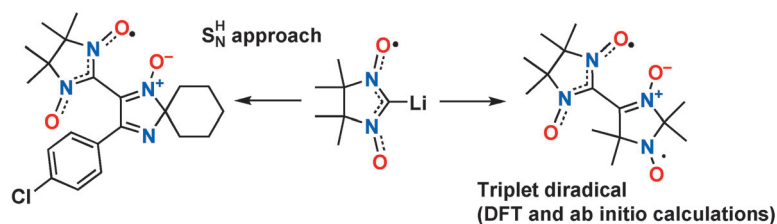
FULL PAPER

Diradicals

S. E. Tolstikov, E. V. Tretyakov,*
D. E. Gorbunov, I. F. Zhurko, M. V. Fedin,
G. V. Romanenko, A. S. Bogomyakov,
N. P. Gritsan, D. G. Mazhukin*



 **Reaction of Paramagnetic Synthon, Lithiated 4,4,5,5-Tetramethyl-4,5-dihydro-1H-imidazol-1-oxyl 3-oxide, with Cyclic Aldonitrones of the Imidazole Series**



Being double: Cyclic aldonitrones undergo nucleophilic substitution of the hydrogen atom with a paramagnetic

carbanion, the lithium derivative of 4,4,5,5-tetramethyl-4,5-dihydro-1H-imidazol-1-oxyl 3-oxide (see scheme).